Chen *et al. Dis Prev Res* 2023;2:16
DOI: 10.20517/dpr.2023.23

Disaster Prevention and Resilience

Research Article

Open Access

Check for updates

Repair procedure-based recovery pattern for estimating seismic resilience and novel concept of public resilience

Xu Chen[1,2], Zhongguo Guan[1,2], Jianzhong Li[1,2], Yutao Pang[3]

[1]Department of Bridge Engineering, Tongji University, Shanghai 200092, China.
[2]State Key Laboratory for Disaster Reduction in Civil Engineering, Tongji University, Shanghai 200092, China.
[3]College of Engineering, China University of Geosciences, Wuhan 430074, Hubei, China.

Correspondence to: Dr. Yutao Pang, College of Engineering, China University of Geosciences, No. 388 Lumo Road, Wuhan 430074, Hubei, China. E-mail: pangyutao@cug.edu.cn

How to cite this article: Chen X, Guan Z, Li J, Pang Y. Repair procedure-based recovery pattern for estimating seismic resilience and novel concept of public resilience. *Dis Prev Res* 2023;2:16. https://dx.doi.org/10.20517/dpr.2023.23

Received: 3 Jul 2023 **First Decision:** 7 Aug 2023 **Revised:** 5 Sep 2023 **Accepted:** 18 Sep 2023 **Published:** 26 Sep 2023

Academic Editor: Yongbo Peng **Copy Editor:** Fangling Lan **Production Editor:** Fangling Lan

Abstract

This study proposes a repair procedure-based recovery pattern for better estimation of structural seismic resilience, which is scarcely considered in previous studies. In this manner, the multiple repair stages and detailed repair sequences of each damaged component are incorporated into the post-earthquake structural functionality, which could better present the recovery process. Additionally, to indicate the structural resilience from the point of public civilians, a novel concept of public resilience (PR) is proposed as well. In this concept, the functionality of structures remains zero until they are completely repaired and opened to the public. This is because, for civilians, the structural functionality is meaningless before opening for full utilization. Analytical analysis and numerical illustrative examples of typical highway bridges are utilized, demonstrating the efficiency of the proposed concepts. The results show that even for the simplified situation with only two damaged components, the seismic resilience is substantially affected by incorporating the stages and the sequences of repair procedures. While for more complex practical scenarios, the influence of repair procedures is expected to be more significant. Additionally, since the recovery pattern of PR is represented through stepwise functions, the value of PR is always lower than that of conventional methods. This fact indicates that for public civilians, seismic resilience of structures will not be as high as that in the view of engineers and researchers.

Keywords: Seismic resilience, repair procedure-based, recovery pattern, repair sequences, public resilience

INTRODUCTION

Earthquakes rank among the most devastating natural disasters for human beings, which destroy structures and cause extensive life and financial losses (e.g., the 2008 Wenchuan earthquake and the 2011 Tohoku earthquake)[1,2]. Of particular concern is the vulnerability of bridges, which are crucial nodes in transportation networks during earthquakes. Besides the direct losses caused by repairing and rebuilding, the damage of bridges can also lead to enormous indirect life and financial losses due to the interruptions of network connectivity[3,4]. Thus, ensuring that bridges can rapidly restore functionality is essential for post-disaster rescue operations. However, the current seismic design concept of bridges generally concentrates on their performance during earthquakes, while the post-disaster functionality is scarcely considered in specifications.

In recent decades, the concept of resilience has been proposed and has become one of the main focuses of new trends in performance-based design of critical structures and infrastructure systems[5]. Generally, resilience means the ability of individual structures, infrastructure systems, and whole region communities to resist disasters and recover to their pre-disaster functionality[6]. One of the most widely accepted manners for quantifying the seismic resilience (R) is expressed as follows[7,8]:

$$R = \frac{1}{t_h - t_0} \int_{t_0}^{t_h} Q(t)dt \tag{1}$$

where t_0 indicates the occurrence of an earthquake event; t_h shows the end of the period considered for analysis; $Q(t)$ means the structural functionality at time t, which is further illustrated in Figure 1.

In Figure 1, t_s and t_c are the moments indicating initiation and completion of recovery procedures; thus, the seismic resilience R is the area under the recovery function profile averaged on the time period (t_0, t_h). From this Equation and Figure, the expression of $Q(t)$ remains one of the most significant factors that determine the computed seismic resilience R. However, in most investigations to date, $Q(t)$ is considered a continuous function with an assumed format[9-11]. This treatment, which might be meaningful mathematically, needs to be improved for practical engineering applications. For example, multiple components could be damaged during earthquakes, and thus, various repair stages occur in recovery practice; further, the detailed sequences of repairing each component may vary due to the whole retrofit plans. All these factors affect the shape of $Q(t)$ and thus lead to substantial variation of computed R values. On the other hand, a few studies have been conducted with non-continuous functions, representing the recovery of structural functionality[12,13]. Mitoulis *et al.*, among others, utilized stepwise functions to consider the capacity restoration of bridges damaged during floods and, thus, evaluate the corresponding resilience[14].

This study proposes a novel repair procedure-based recovery pattern for the computation of structural seismic resilience. In this manner, the multiple stages and detailed sequences of repair procedures are incorporated in the expression of structural functionality $Q(t)$ to better represent the post-earthquake recovery process of damaged structures. Additionally, a new concept of public resilience (PR) is also proposed, indicating the restoration of structures for public utilization, i.e., representing the resilience from the point of civilians. Both analytical and numerical analysis are utilized, verifying the efficiency of the proposed repair procedure-based recovery pattern and PR. The corresponding results can serve as foundations for further investigations, providing more realistic estimations of seismic resilience, which may finally lead to resilience-based seismic engineering.

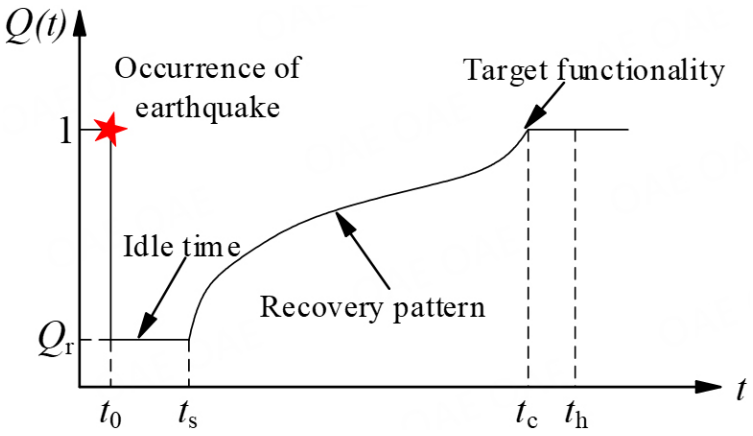

Figure 1. Illustration of functionality, $Q(t)$.

NOVEL RECOVERY PATTERNS FOR STRUCTURAL RESILIENCE ASSESSMENT

From the aforementioned studies, current procedures assessing the seismic resilience might be insufficient in several aspects: (1) the damage states currently utilized to determine the recovery patterns are mainly those of the whole structural systems rather than individual components; (2) the recovery pattern is represented by simple continuous functions without considering the details in repair procedures.

Consequently, this section presents the attempt to associate the structural resilience (SR) with the damage of each individual component and the specific repair procedures adopted in practice.

Recovery pattern with damaged component and repair procedure

As mentioned previously, various types of recovery patterns have been proposed and applied in previous investigations, which are substantially related to the damage states of structure systems. Nevertheless, even when the system-level structural damage remains identical, the repairing procedures and the corresponding recovery patterns can be significantly different if the state is dominated by different individual components. This fact has been intentionally or unintentionally realized by some researchers but not fully clarified; for example, Lian *et al.* utilized the component fragility to calculate the repair cost instead of the system one, which indicated that the repair procedure and corresponding cost were dominated by the damage of each component[15]. The following two reasons mainly contribute to this issue:

(1) The repair details of each component follow certain specific rules. Using a bridge system for illustration, retrofitting damaged columns, bearings, or girders involves quite different procedures. Consequently, the time consumption, financial cost, and even recovery pattern function of the whole bridge systems may vary substantially even if the bridges are identified with the same level of damage but dominated by different components. For example, the complete damage state of one bridge system can be caused by either collapse of columns or falling-off of girders; however, the recovery procedures for these two scenarios are certainly different.

(2) The repair procedures generally depend on the characteristics of structural systems (e.g., types and locations). For example, the restoration process of bridges located in deep-water environments (e.g., reservoirs) is more complex and costly than that of the urban highway bridges[16]. Additionally, while the micro cracks in conventional bridges may not be that significant, they should be carefully considered for underwater piers since these cracks can substantially accelerate the corrosion of steel bars and, thus,

deteriorate the structural durability. Thus, an extra step of curing micro cracks with underwater concrete might be further required to repair underwater piers[17].

Additionally, the recovery patterns are generally assumed to be continuous functions, with the formats and critical parameters determined according to the experience of engineers[18,19]. However, these functions are scarcely validated since limited data on practical projects are available to date. Note that the repair process substantially depends on factors such as the organizational capacity of local government, the abilities of construction companies, and the plans for rescue and restoration. Therefore, neglecting specific details of repair procedures in recovery patterns may not be proper.

Based on the above statement, the current study proposes that the recovery patterns utilized to determine the SR should incorporate the influence of the detailed repair process of specific structures, as presented in Figure 2:

(1) the parameters and/or format of the recovery pattern function for each component should be determined according to their damage state, as presented in Figure 2A; Δt_1 and Δt_2 indicate the repair time for components 1 and 2, Δt_{I1} and Δt_{I2} mean the corresponding idle time, while ΔQ_1 and ΔQ_2 are the improvements of structural functionality when the two components are repaired.

(2) the recovery pattern functions of the damaged components should be considered in different sequences according to the repair plan of the structure, as shown in the two illustrative examples in Figure 2B. The resilience of the two cases shown in this figure will certainly be different if the recovery patterns of the two components are different, although the repair work starts (t_s) and completes (t_c) simultaneously.

Comparison with conventional recovery pattern

To better present the features of the proposed recovery pattern, qualitative comparisons are briefly provided in this sub-section for illustration. The seismic resilience is computed using both the novel and conventional recovery patterns, implying the significance of considering repair procedures. Then, the influence of the specific repair sequence of each component is demonstrated by considering two simple recovery patterns that are identical except for the detailed repair sequence.

Note that the current investigation is a preliminary study that mainly aims to propose a concept of novel recovery patterns that can account for the effects of detailed repair procedures in assessing seismic resilience. Consequently, the procedure considered hereafter will only incorporate two repair stages for illustrative purposes; for more complicated practical projects that would include multiple procedures, the recovery patterns might be developed with the help of a construction organization chart that represents the whole repair process in practice. Furthermore, the recovery process of functionality will be simplified as linear hereafter. In real projects, both the format and critical time (i.e., $Q(t)$ - t relation) of recovery remain subjects requiring further investigation, and these aspects can only be determined according to current expert suggestions.

Influence of incorporating repair procedure

Figure 3 provides three examples of damaged structures with different repair procedures, which may be caused by either the change of component that dominates damage states or the specific repair sequence of various components. The red lines represent the recovery pattern commonly employed in available investigations, neglecting the repair details and regarding the recovery as a whole process, while the black lines are those proposed herein considering repair stages. In this figure, the ΔQ denotes the improvement of

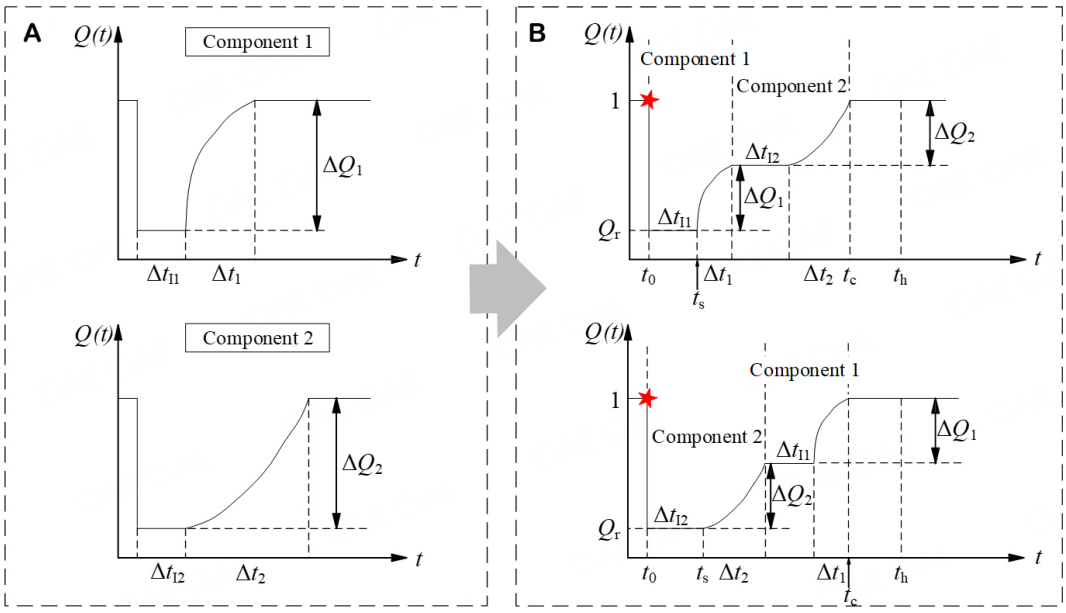

Figure 2. Illustrative repair procedures for different bridge components: (A) Recovery patterns for individual components; (B) system recovery with different repair sequences.

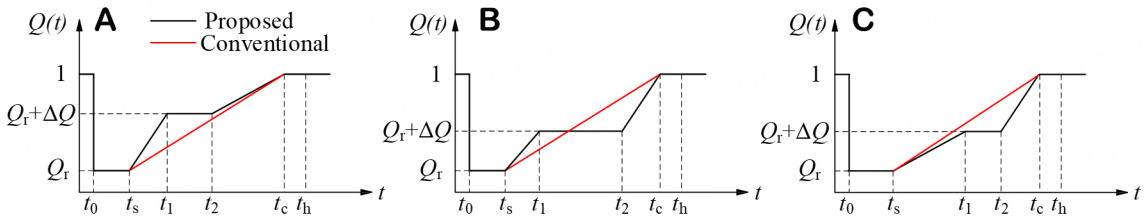

Figure 3. Illustrative examples showing the influence of incorporating repair procedures, in which the proposed is (A) Exceeding, (B) crossing, and (C) beneath the conventional.

functionality at the completion of the first repair stage; t with various subscripts indicates the critical time points. Note that except for the start and end of the time period considered for analysis, i.e., t_0 and t_h, all the other parameters in these three scenarios could be different.

Figure 3 demonstrates that while the residual functionality Q_r, target functionality Q_t (usually equal to 1.0), and the time period (t_0, t_h) are specified, the resilience R is correspondingly determined in conventional methods. However, for the repair procedure-based recovery patterns proposed in the current study, R values are related to various factors, e.g., the functionality after repairing certain components ($Q_r + \Delta Q$) and the time consumption of individual repair stage (t_1 - t_0 or t_c - t_1). Depending on the recovery patterns, the repair-based resilience can be either greater (e.g., Figure 3A) or less (e.g., Figure 3C) than the conventional ones.

For better comparison and understanding, the seismic resilience values corresponding to the conventional and proposed recovery pattern, as shown in Figure 3B, are calculated as follows for illustration, denoted as R_c and R_p, respectively.

$$R_c = \frac{1}{t_h - t_0}\left(\left(-t_0 + \frac{t_s}{2} + \frac{t_c}{2}\right)Q_r + \left(-\frac{t_s}{2} - \frac{t_c}{2} + t_h\right)\right) \quad (2)$$

$$R_p = \frac{1}{t_h - t_0}\left(\left(-t_0 + \frac{t_s}{2} + \frac{t_1}{2}\right)Q_r + \frac{1}{2}(-t_s - t_1 + t_2 + t_c)(Q_r + \Delta Q) + \left(-\frac{t_2}{2} - \frac{t_c}{2} + t_h\right)\right) \quad (3)$$

The difference (ΔR) between R_c and R_p can be obtained as Eq. (4), in which t_0, t_s, t_c, t_h, and the residual functionality Q_r are assumed identical in these two recovery patterns for simplicity and better comparison. This Eq. (4) reveals that the conventional method can either overestimate or underestimate the resilience, depending on the details of repair processes, namely the time corresponding to the completion of repairing the first component (t_1) and the initiation of repairing the second one (t_2), as well as the improvement of functionality (ΔQ) at t_1.

$$\Delta R = R_c - R_p = \frac{1}{2(t_h - t_0)}[(t_2 - t_s)(1 - Q_r - \Delta Q) - (t_c - t_1)\Delta Q] \quad (4)$$

Influence of repair sequence of damaged components

This subsection aims to further interpret the influence of repair sequences of different components shown in Figure 2B in a quantitative manner using simplified recovery patterns. Figure 4 provides two illustrative examples with two identical repair stages but in different sequences. In these situations, the time consumptions of two repair stages are denoted as Δt_1 and Δt_2, respectively, while the idle time are both assumed as Δt_I; the improvement of functionality is considered as ΔQ_1 and ΔQ_2. Note that although the critical time during recovery (t_1 and t_2 *vs.* t_1' and t_2') are different in these two examples, the time indicating the completion of the whole process and for analysis is identical (i.e., t_c and t_h).

Similar to Eqs. (2-4), the resilience corresponding to Figure 4A and B is computed as follows in Eqs. (5) and (6), denoted as R_a and R_b, respectively; the difference ΔR (= R_a - R_b) is presented in Eq. (7). These equations imply that the sequences of repair work affect the SR through their duration and improvement of functionality; while the idle time Δt_I for various stages is considered different, it influences the assessment as well.

$$R_a = \frac{1}{t_h - t_0}\left(\left(-t_0 + \frac{t_s}{2} + \frac{t_1}{2}\right)Q_r + \frac{1}{2}(-t_s - t_1 + t_2 + t_c)(Q_r + \Delta Q_1) + \left(-\frac{t_2}{2} - \frac{t_c}{2} + t_h\right)\right) \quad (5)$$

$$R_b = \frac{1}{t_h - t_0}\left(\left(-t_0 + \frac{t_s}{2} + \frac{t_1'}{2}\right)Q_r + \frac{1}{2}(-t_s - t_1' + t_2' + t_c)(Q_r + \Delta Q_2) + \left(-\frac{t_2'}{2} - \frac{t_c}{2} + t_h\right)\right) \quad (6)$$

$$\Delta R = R_a - R_b = \frac{1}{2(t_h - t_0)}\left((\Delta t_2 - \Delta t_1)(1 - Q_r) + (-t_s + \Delta t_I + t_c)(\Delta Q_1 - \Delta Q_2)\right) \quad (7)$$

CONCEPT OF PUBLIC RESILIENCE

Note that almost all the provided studies on SR utilize the continuous functions that are monotonically increasing to present the recovery pattern to date, regardless of the damage states. This assumption is reasonable from the standpoint of structural engineering since the structural integrity and functionality gradually improve with the advancing of repair procedures and finally reach the objective performance once completed. However, this procedure is totally a different story to the public civilians who utilize the infrastructures for living (residential buildings) or commuting (bridges or roads) in daily life. From their perspective, the service functionalities of all the structures remain zero until the accomplishment of repairs and then suddenly change to unity, i.e., opening for full utilization[14].

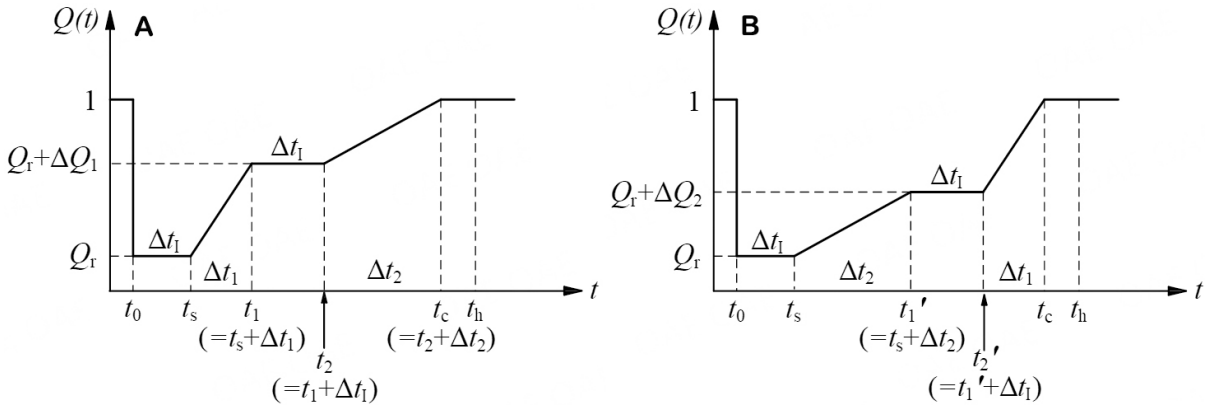

Figure 4. Illustrative examples showing the influence of repair sequence: (A) ΔQ_1 required first; (B) ΔQ_2 repaired first.

Therefore, we propose a novel concept of public resilience (PR) in the current study to replace the SR for the social application value, which differentiates from the traditional resilience considered by designers and engineers. This PR concept is especially substantial for policy makers because it can help to propose rescue plans prior to earthquake events, which will considerably reduce the potential financial and life loss. Additionally, PR is significant for civilians since this parameter indicates the restoring procedure of structures (and maybe the whole social life) and their access to re-utilization of the structures damaged during earthquakes.

As the comparison presented in Figure 5A, the SR of the damaged structure gradually increases with the repair process, while PR jumps to unity at the completion of repair. Note that multiple steps may be contained in PR in specific scenarios; for example, bridges damaged during earthquakes can be partly opened to the public for controlled traffic load, and thus, PR can be represented by the multi-stepwise function, as shown in Figure 5B. From both scenarios, PR is observed lower than SR; mathematically, SR is the theoretical upper limit of PR. This phenomenon is reasonable that the recovery of structural functionality is the prerequisite of public utilization, and thus, PR can never be greater than SR.

ILLUSTRATIVE EXAMPLES

This section provides simple illustrative examples for assessing the structural resilience in various manners, including SR through the conventional and the proposed repair procedure-based pattern, as well as PR. The prototype bridge is first introduced, followed by the selected ground motions and damage states. Then, both the SR and PR are obtained and compared with the resilience computed.

Bridge prototype and finite element model

A typical highway bridge shown in Figure 6 is employed as the prototype. The superstructure of this bridge is composed of three 35 m-length spans, each weighing 800 t, seating on rubber bearings placed at the top of cap beams. Shear keys are implemented on the cap beams to restrict the transversal movement of the girders. Single circular columns are constructed with diameter and height of 1.6 m and 10 m, respectively. The axial compression force at the pier base is 8,500 kN, leading to an axial load ratio of 0.15. The pier columns are integrated with expanded foundations with dimensions of 5 m × 5 m. For simplicity, only the dynamic responses in longitudinal direction are computed and discussed in the following sections.

According to the Chinese Code for Seismic Design of Urban Bridges[20], the seismic behavior of this bridge can be represented by one column and is dominated by the fundamental vibration mode. Therefore, it can

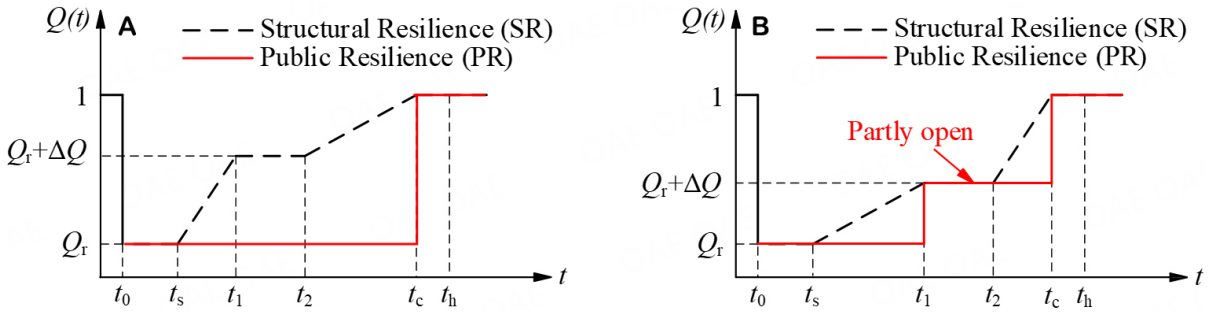

Figure 5. Illustration for recovery patterns of (a) PR and SR; (b) multi-step PR.

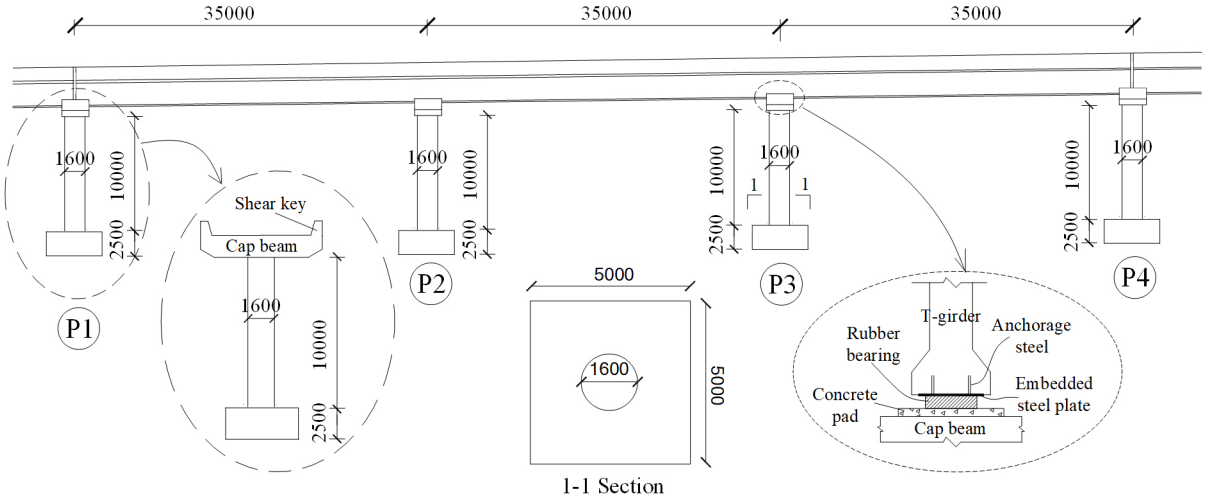

Figure 6. Background (prototype) bridge (unit: mm) .

be simplified as an SDOF system, and the corresponding finite element model developed using the OpenSees platform is shown in Figure 7. The capacity-protected superstructure is represented by a lumped mass at the column top (m = 820 t), which accounts for the mass of two adjacent half-spans and the equivalent mass of the pier column[20].

Since the rubber bearings are usually directly placed between the girder base and column top in typical highway bridges in China, a flat slider bearing element is, therefore, employed to account for the potential sliding during excitation. The friction effect is considered by the Coulomb friction model with a friction coefficient μ of 0.35[21,22]. To consider the nonlinearity during strong shakings, pier columns are simulated through fiber elements, in which the sections are discretized as cover/core concrete fibers and steel fibers according to the different materials and confinement conditions[23,24]. The constitutive relation of concrete is determined according to the Mander model[25], while the bilinear model[26,27] is used to present the steel bars; detailed information on the material parameters is shown in Figure 7. Note that only the compression behavior of concrete is considered in this model since the tensile capacity is quite small compared with compression and will not contribute much to the structural resistance during earthquakes.

Selected ground motions and damage state

Recent investigations indicate that compared with far-field motions commonly considered in current codes, near-fault ones may lead to more significant damage to bridges[28-30]. Therefore, 40 near-fault motions

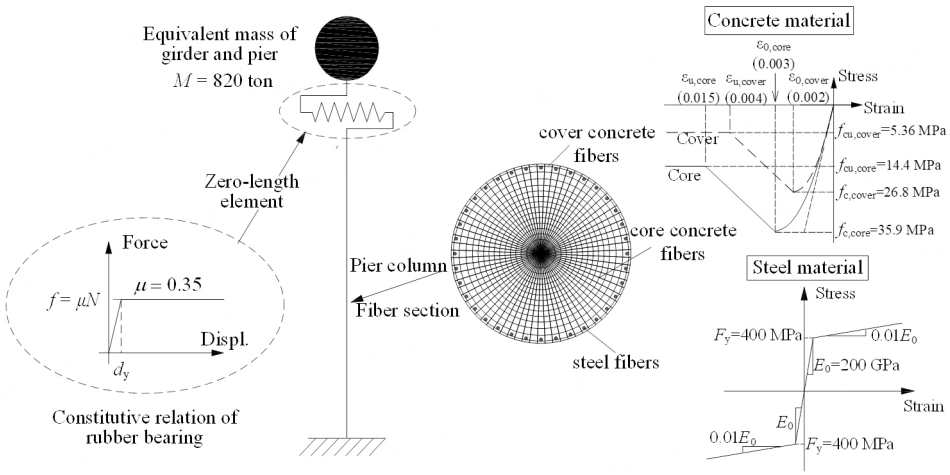

Figure 7. Finite element model of the prototype.

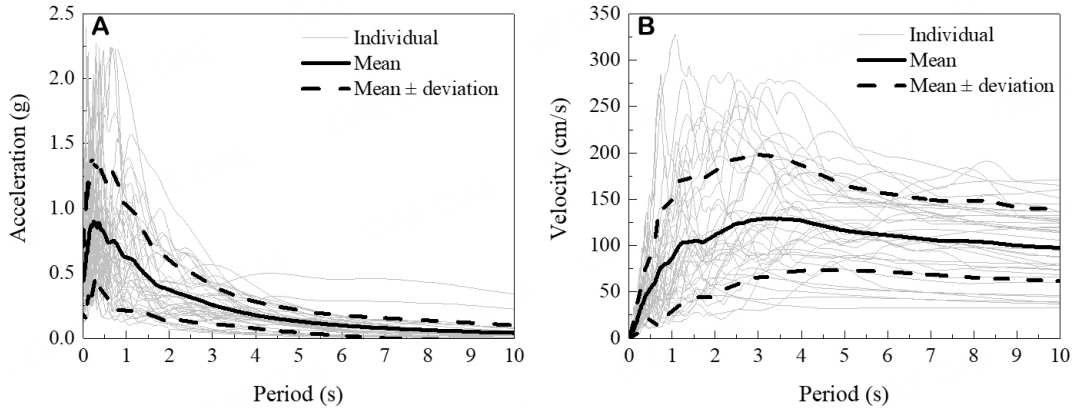

Figure 8. Spectra of the selected motions (5% damping): (A) Acceleration; (B) velocity.

selected from the PEER database and presented in the previous study are utilized as input herein. The peak ground acceleration (PGA) and peak ground velocity (PGV) of these motions are from 0.13 g to 1.34 g and from 32.85 cm/s to 348.82 cm/s, respectively, covering wide cases from slight to catastrophic earthquakes. The corresponding acceleration and velocity spectra of each individual motion are shown in Figure 8, where the mean values and the mean ± standard deviation ones are plotted as well. More detailed information can be found in[31].

To generate sufficient data for assessing the seismic fragility that is necessary for further evaluation of resilience, all 40 motions are scaled by three factors (0.5, 1.0, and 1.5), composing a set of 120 inputs. Note that greater scalars are not utilized since they are thought to lead to excitations with unrealistic frequency characteristics[32].

To characterize the damage to the bridge, four damage states, namely, slight, moderate, extensive, and complete, are usually employed to assess the seismic performance of structures for both component and system levels. In this study, rubber bearings and pier columns are considered as vulnerable components, with the states characterized by shear deformation (d) and section curvature (μ_ϕ), respectively. The thresholds suggested by previous investigations are utilized for each damage state, as listed in Table 1[33,34].

Table 1. Damage states for columns and bearings

Component	Damage index	Damage limit state			
		Slight	Moderate	Extensive	Complete
Bearing	Shear deformation, d (mm)	$d > 28.9$	$d > 104$	$d > 136$	$d > 187$
	S_c	28.9	104	136	187
	β_c	0.60	0.55	0.59	0.65
Column	Curvature ductility, μ_ϕ	$\mu_\phi > 1.29$	$\mu_\phi > 2.10$	$\mu_\phi > 3.52$	$\mu_\phi > 5.24$
	S_c	1.29	2.1	3.52	5.24
	β_c	0.59	0.51	0.64	0.65

To determine the system-level damage states that are required to compute the seismic resilience in conventional methods, the manner suggested by Zhang and Huo[35] is adopted herein. In this method, the system is considered to have reached complete damage when either the column or bearing reaches a complete state of damage; otherwise, it is determined by assigning weights to the states of the column and bearing as follows:

$$\mathrm{DS}_{\mathrm{sys}} = \begin{cases} \mathrm{int}(0.75\mathrm{DS}_{\mathrm{col}} + 0.25\mathrm{DS}_{\mathrm{bear}}) & \mathrm{DS}_{\mathrm{col}},\ \mathrm{DS}_{\mathrm{bear}} < 4 \\ 4 & \mathrm{DS}_{\mathrm{col}}\ \&\ \mathrm{DS}_{\mathrm{bear}} = 4 \end{cases} \tag{8}$$

where $\mathrm{DS}_{\mathrm{sys}}$, $\mathrm{DS}_{\mathrm{col}}$, and $\mathrm{DS}_{\mathrm{bear}}$ are the damage states of the system, column, and bearing, which equal 1, 2, 3, and 4 for the slight, moderate, extensive, and complete damage, respectively.

Seismic resilience assessment

Seismic fragility

Seismic fragility analysis is the prerequisite for obtaining the corresponding resilience[36]. Based on the near-fault ground motions and damage states provided in Section "Selected ground motions and damage state", the fragility curves for the pier, bearing, and bridge system are obtained, as shown in Figure 9. In this figure, the PGV is utilized as the intensity measure (IM) in the horizontal axis since it is recognized as a representative characteristic of near-fault motions[23,32]. Note that the fragility results of components, i.e., those in Figure 9A and B, are obtained through cloud methods[37], while those shown in Figure 9C for the whole system are computed using Mento Carlo simulations based on the component-level results and Eq. (8).

This figure shows that the bearing is more sensitive to slight damage than the pier column, while for the other three damage states, the pier column becomes more vulnerable. Additionally, for the fragility of the bridge system presented in Figure 9C, the extensive damage state curve almost coincides with the complete damage one. The reason is that the system is specified as completely damaged once either the bearing or pier reaches complete damage states as in Eq. (8); thus, samples generated in Mento Carlo simulations with $\mathrm{DS}_{\mathrm{sys}} = 4$ are substantially more than $\mathrm{DS}_{\mathrm{sys}} = 3$.

Seismic resilience

To better present the traits of the resilience in the proposed manner, four scenarios are considered and compared for resilience assessment:

Scenario 1 (S1): resilience in a conventional manner, i.e., utilizing the recovery pattern determined according to the damage states of the whole bridge system based on Eq. (8), as shown in Figure 10A;

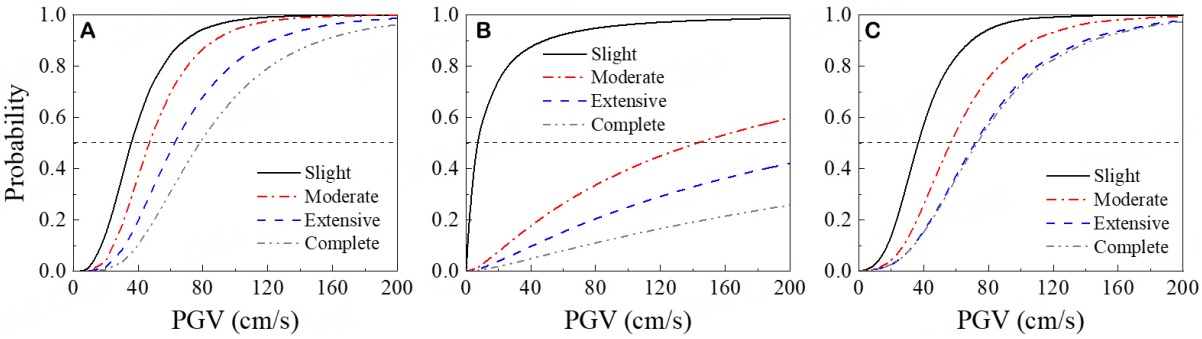

Figure 9. Fragility curves of (A) Pier; (B) bearing; (C) bridge system.

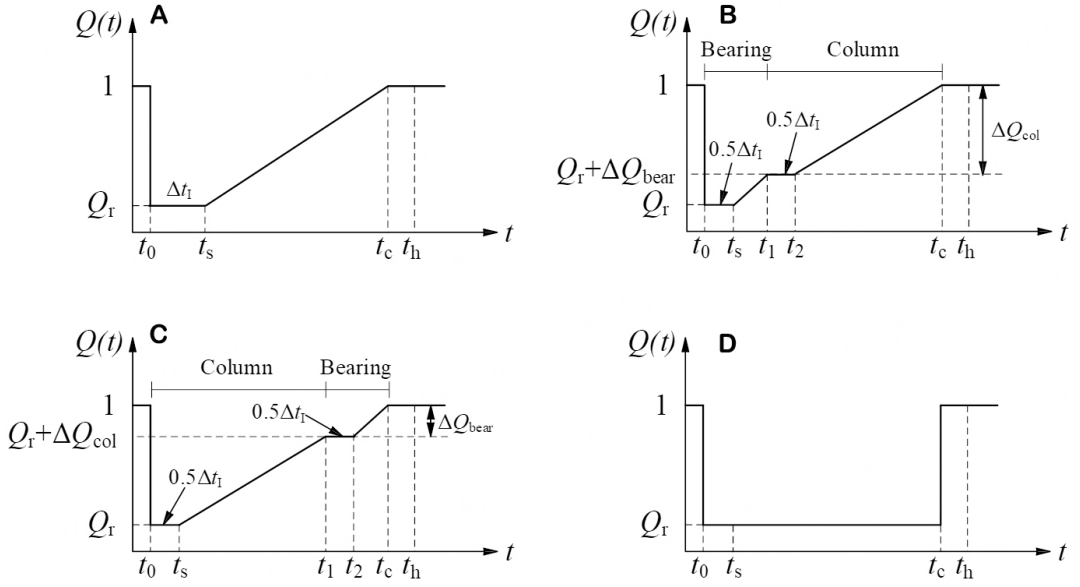

Figure 10. Considered scenarios for resilience from (A) Conventional manner; (B) repair procedure-based with "*bearing → column*" sequence; (C) repair procedure-based with "*column → bearing*" sequence; and (D) Public resilience.

Scenario 2 (S2): resilience using repair procedure-based recovery patterns, with repair sequence of "*bearing → column*", as shown in Figure 10B;

Scenario 3 (S3): resilience using repair procedure-based recovery patterns, with repair sequence of "*column → bearing*", as shown in Figure 10C;

Scenario 4 (S4): the PR, assuming the bridge fully opened to the public after the repair of both components completed, as shown in Figure 10D.

Note that in engineering practice, realigning of bearings may generally follow the completion of repairing columns, i.e., the sequence in S2 may not be the actual situation; however, the main purpose of this scenario is to indicate the influence of repair sequence through comparing with S3.

Parameters for analysis

For simplicity, the uncertainties concerning the functionality $Q(t)$ are not incorporated herein. In other words, we consider the residual functionality Q_r and the improved functionality after repair of bearing ΔQ_{bear} and column ΔQ_{col} as deterministic values. For slight, moderate, extensive, and complete damage to the bridge system, Q_r is assumed as 0.1, 0.4, 0.7, and 0.9, respectively, as suggested in reference[9]. When determining ΔQ_{bear} and ΔQ_{col}, Eq. (8) indicates that piers are generally recognized as more significant than bearings for the state of bridge systems. Therefore, ΔQ_{bear} and ΔQ_{col} are assumed to account for 25% and 75% of the lost functionality, respectively, i.e., $\Delta Q_{bear} = 0.25(1 - Q_r)$ and $\Delta Q_{col} = 0.75(1 - Q_r)$. Furthermore, to provide a fair comparison, the total time period for analyzing seismic resilience, i.e., $t_h - t_0$, is assumed as 300 days for all the scenarios.

On the other hand, the uncertainties related to the time period of recovery patterns are considered. For S1, as shown in Figure 10A, the recovery pattern only depends on two variables, i.e., the idle time Δt_I and the repair period $t_c - t_s$. These two variables are assumed to follow uniform distributions, as suggested in reference[11]. For a fair comparison, $t_c - t_s$ in S2 and S3 is assumed identical as in the case of S1, while the idle time is split into two intervals of $0.5\Delta t_I$, as shown in Figure 10B and C, because two repair stages are considered in these two scenarios. The duration of repairing bearing (Δt_{bear}) is assumed to follow uniform distributions[38], and thus, that of a column, Δt_{col}, is computed as ($t_c - t_s - \Delta t_{bear} - 0.5\Delta t_I$) to ensure the consistency of total repair time. Details of these parameters are listed in Table 2[11].

Comparisons of recovery patterns and resilience index

For the resilience analysis, 21 PGV intensities from 0 up to 200 cm/s are considered, with intervals of 10 cm/s. To ensure the reliability of the results, 10^6 samples are generated for each PGV level, and the averaged values are utilized for analysis. Figure 11 shows and compares the recovery patterns, i.e., expected functionality *vs*. recovery time t, for all four scenarios corresponding to several illustrative PGV intensities. Once the input PGV is specified, all the scenarios are observed with identical residual functionality Q_r. This phenomenon is reasonable that Q_r is determined by the damage state of bridge systems, which is specified considering the states of both bearings and columns according to Eq. (8). Additionally, Q_r decreases with the increase of PGV, since more intensive earthquakes are expected leading to more severe damage and lower residual functionality.

Note that the recovery patterns of S3 are shown to be quite similar to those of S1 in the current study. The reason is that when the recovery procedure is regarded as a whole in the conventional manner (i.e., S1), it is inherently a mixture of repairing bearings and columns. The repair of columns generally dominated the recovery pattern herein in terms of both contribution to functionality ($\Delta Q_{col} = 3\Delta Q_{bear}$) and recovery time [Table 2]. Consequently, while the column is repaired prior to bearing in S3, the structural functionality generally recovers, similar to that of S1. Additionally, since the idle time before the repairing column is half of that in S1 [Table 2], the functionality in S3 starts to recover earlier than S1.

On the other hand, the functionality of S2 is always greater than the above two scenarios throughout the recovery time. This phenomenon is caused by the fact that the bearing is assumed to be realigned first in this scenario, and thus, the repair procedure of the column, which accounts for most recovery time and improvement of functionality, initiates at a higher functionality level than in the case of S3. This situation will certainly lead to higher resilience of S3, which will be further presented in the following parts.

For S4, the functionality is consistently lowest as expected, because it is considered to remain as Q_r until the completion of the whole repair procedure, as shown in Figure 10D. Note that the functionality

Table 2. Parameters for restoration process in conventional resilience assessment

Damage state	$t_c - t_s$ (days)		Δt_I (days)		Δt_{bear} (days)		Δt_{col} (days)
	Min	Max	Min	Max	Min	Max	
Slight	5	120	5	30	3	8	$t_c - t_s - \Delta t_{bear} - 0.5\Delta t_I$
Moderate	15	170			3	8	
Extensive	55	220			5	10	
Complete	75	270			5	10	

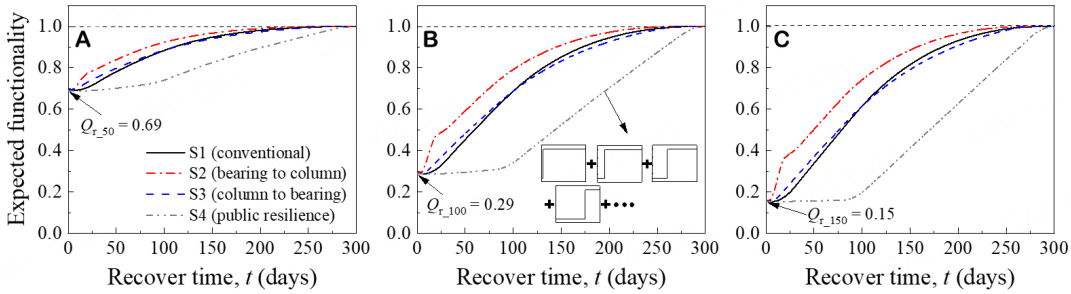

Figure 11. Recovery patterns for PGV of: (A) 50 cm/s; (B) 100 cm/s; (C) 150 cm/s.

approximately rises linearly once the recovery time exceeds certain values. The reason is that because both $t_c - t_s$ and Δt_I are assumed to follow uniform distributions, as shown in Table 2, the time when functionality jumps to 1.0 will uniformly occur in a certain range. Therefore, the averaged results presented in Figure 11 show a linear increasing tendency.

Figure 12 further presents the resilience index R with respect to the input PGV for all four considered scenarios. Coincident with the recovery patterns plotted in Figure 11, S2 always shows the highest resilience and S4 the lowest, while the other two scenarios remain quite similar. Note that even for the simplified illustrative examples utilized herein, the resilience can vary substantially in different scenarios. Using the results corresponding to PGV of 120 cm/s as examples, the resilience estimated by S3 can be 10% greater than that of conventional manner (S1), while the result of S4 is only about 70% of S1.

DISCUSSIONS

The aforementioned analytical results demonstrate that even for the simplified illustrative examples only with two damaged components (i.e., bearing and column), the SR can be substantially influenced once the repair sequence is changed (S2 *vs.* S3). For engineering structures with more vulnerable components and, thus, more complicated repair procedures, only determining recovery patterns that depend on damage states while neglecting the detailed repair procedure can lead to significant errors, either overestimating or underestimating resilience.

Since both the recovery pattern and resilience of S3 are quite similar to those of S1, the conventional manner can be inferred as inherently assuming that the pier column dominates the structural damage states and is repaired first during the recovery procedures, which might be reasonable in the current example. However, this assumption will be questionable for a more complex practical situation. Particularly in more general scenarios, the column in the current examples can be regarded as the component that most significantly contributes to the damage state and functionality of a structure. The detailed sequence of repairing each damage component may be affected by various factors, such as the availability of workers and engineering machines and the potential requirements of the public and government.

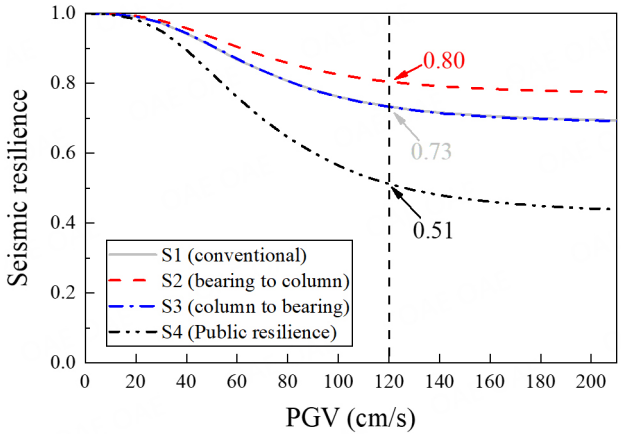

Figure 12. Seismic resilience *R vs.* PGV.

Additionally, the linear increase part of recovery patterns in S4, i.e., PR, is due to the assumed uniform distribution of t_c - t_s and Δt_i; that is, the shape of this part that significantly affects the calculation of the resilience index depends on the distribution patterns of repair time. Therefore, more work should be conducted to provide reliable estimation of the repair time, which might be determined through recording detailed data for real retrofitting projects and/or collecting opinions of engineers with questionnaires.

Note that the PR proposed here mainly focuses on the resilience estimated from the point of public civilians; that is, PR is expected to represent the ability of civilians to re-access and re-use the structures (e.g., bridges, buildings, roads, *etc.*) damaged in earthquakes. However, this concept is quite different from community resilience, which considers the resilience at a regional level, and the interaction and relations among various structures in the investigated region are substantial[39,40]. For example, when estimating the community resilience for a city, the integrity and connectivity of the whole highway network are crucial, in addition to evaluating the PR of a single structure (e.g., bridge).

The repair procedure-based recovery pattern and the concept of PR are both preliminary proposed and investigated in the current study. Extensive future work is required concerning various issues, including determining the improvement of structural functionality and the time required once a certain component is repaired, searching for the optimal repair procedure to maximize the seismic resilience, and proposing a convenient PR-based framework informing the public about the resilience of structures. Furthermore, utilizing proper realistic applications (e.g., base isolation[41] and geotechnical seismic isolation (GSI) technique[42]) to enhance the seismic performance of bridges is another significant issue for the ultimate objective of improving resilience.

CONCLUSIONS

This paper investigates the influence of repair procedures on the structural seismic resilience, based on which suggests the utilization of repair procedure-based recovery patterns for the estimation of resilience. Additionally, the novel concept of PR is proposed to indicate the restoration of structural functionality that is meaningful to the decision-makers and/or the public rather than the professional engineers. Based on analysis, the following conclusions and findings are obtained:

1 Through an analytical manner, the seismic resilience is demonstrated substantially influenced by the duration and improvement of functionality of each component in repair procedures. Furthermore, the

detailed sequence of repairing damaged components affects the obtained resilience as well.

2 Simplified illustrative examples of typical highway bridges show that even for the situations with only two damage components, the seismic resilience is significantly affected once the repair procedure is changed. Especially for the catastrophic earthquakes with high intensity, the variation of estimated resilience can be greater than 10%. While for more complicated practical structures, incorporating repair procedures during resilience analysis is expected to be more substantial.

3 The commonly employed recovery patterns of structural functionality represented by continuous function may be reasonable in the view of engineers, which accounts for the improvement of structural integrity with the repair procedure. However, for civilians, the infrastructure is not considered functional till the repair work is accomplished and opened for access or utilization.

4 The recovery patterns of the proposed PR are stepwise functions instead of continuous ones; the functionality remains on a constant level during repairing work and jumps to a higher level once part (or whole) of the structures is restored and opened for utilization. Due to its definition, PR is always lower than the SR usually studied, as demonstrated by the numerical results, indicating that public civilians will not consider the resilience of a structure as high as engineers.

DECLARATIONS

Authors' contributions

Conceptualization, data curation, formal analysis, funding acquisition, investigation: Chen X
Conceptualization, writing-review & editing: Guan Z, Li J
Conceptualization, writing-review & editing; methodology: Pang Y

Availability of data and materials

Data will be made available on request.

Financial support and sponsorship

None.

Conflicts of interest

All authors declared that there are no conflicts of interest.

Ethical approval and consent to participate

Not applicable.

Consent for publication

Not applicable.

REFERENCES

1. Xiang N, Li J. Effect of exterior concrete shear keys on the seismic performance of laminated rubber bearing-supported highway bridges in China. *Soil Dyn Earthq Eng* 2018;112:185-97. DOI
2. Yamamoto M, Minewaki S, Yoneda H, Higashino M. Nonlinear behavior of high-damping rubber bearings under horizontal bidirectional loading: full-scale tests and analytical modeling. *Earthq Eng Struct Dyn* 2012;41:1845-60. DOI

3. Zhou Y, Banerjee S, Shinozuka M. Socio-economic effect of seismic retrofit of bridges for highway transportation networks: a pilot study. *Struct Infrastruct Eng* 2010;6:145-57. DOI
4. Decò A, Bocchini P, Frangopol DM. A probabilistic approach for the prediction of seismic resilience of bridges. *Earthq Eng Struct Dyn* 2013;42:1469-87. DOI
5. Bruneau M, Chang SE, Eguchi RT, et al. A framework to quantitatively assess and enhance the seismic resilience of communities. *Earthq Spectra* 2003;19:733-52. DOI
6. Akiyama M, Frangopol DM, Matsuzaki H. Life-cycle reliability of RC bridge piers under seismic and airborne chloride hazards. *Earthq Eng Struct Dyn* 2011;40:1671-87. DOI
7. Pang Y, Wei K, He H, Wang W. Assessment of lifetime seismic resilience of a long-span cable-stayed bridge exposed to structural corrosion. *Soil Dyn Earthq Eng* 2022;157:107275. DOI
8. Biondini F, Camnasio E, Titi A. Seismic resilience of concrete structures under corrosion. *Earthq Eng Struct Dyn* 2015;44:2445-66. DOI
9. Titi A, Biondini F. On the accuracy of diffusion models for life-cycle assessment of concrete structures. *Struct Infrastruct Eng* 2016;12:1202-15. DOI
10. Biondini F, Vergani M. Deteriorating beam finite element for nonlinear analysis of concrete structures under corrosion. *Struct Infrastruct Eng* 2015;11:519-32. DOI
11. Capacci L, Biondini F. Probabilistic life-cycle seismic resilience assessment of aging bridge networks considering infrastructure upgrading. *Struct Infrastruct Eng* 2020;16:659-75. DOI
12. Padgett JE, Desroches R. Bridge functionality relationships for improved seismic risk assessment of transportation networks. *Earthq Spectra* 2007;23:115-30. DOI
13. Mackie KR, Stojadinović B. Post-earthquake functionality of highway overpass bridges. *Earthq Eng Struct Dyn* 2006;35:77-93. DOI
14. Mitoulis SA, Argyroudis SA, Loli M, Imam B. Restoration models for quantifying flood resilience of bridges. *Eng Struct* 2021;238:112180. DOI
15. Lian Q, Zhang P, Li H, Yuan W, Dang X. Adjustment method of bridge seismic importance factor based on bridge network connectivity reliability. *Structures* 2021;32:1692-700. DOI
16. Wei K, Yuan W, Bouaanani N. Experimental and numerical assessment of the three-dimensional modal dynamic response of bridge pile foundations submerged in water. *J Bridge Eng* 2013;18:1032-41. DOI
17. Guan Z, Zhang J, Li J. Multilevel performance classifications of tall RC bridge columns toward postearthquake rehabilitation requirements. *J Bridge Eng* 2017;22:04017080. DOI
18. Karamlou A, Bocchini P. Functionality-fragility surfaces. *Earthq Eng Struct Dyn* 2017;46:1687-709. DOI
19. Kameshwar S, Misra S, Padgett JE. Decision tree based bridge restoration models for extreme event performance assessment of regional road networks. *Struct Infrastruct Eng* 2020;16:431-51. DOI
20. CJJ 166-2011 Code for seismic design of urban bridges. Beijing: Ministry of Housing and Urban-Rural Development of the People's Republic of China; 2011. Available from: https://ebook.chinabuilding.com.cn/zbooklib/book/detail/show?bookID=56396&SiteID=1 [Last accessed on 25 Sep 2023].
21. Caltrans. Seismic design criteria. Sacramento, CA: California Department of Transportation; 2010.
22. Imbsen RA. AASHTO guide specifications for LRFD seismic bridge design. American Association of State Highway Transport Officials, Subcommittee for seismic effects on bridges; 2007. Available from: http://www.ce.memphis.edu/7119/PDFs/AASHTO/2007-03-09GuideSpec.pdf [Last accessed on 25 Sep 2023].
23. Chen X, Xiang N, Guan Z, Li J. Seismic vulnerability assessment of tall pier bridges under mainshock-aftershock-like earthquake sequences using vector-valued intensity measure. *Eng Struct* 2022;253:113732. DOI
24. He Z, Liu W, Wang X, Ye A. Optimal force-based beam-column element size for reinforced-concrete piles in bridges. *J Bridge Eng* 2016;21:06016006. DOI
25. Scott BD, Park R, Priestley MJ. Stress-strain behavior of concrete confined by overlapping hoops at low and high strain rates. *J Process* 1982;79:13-27. DOI
26. Guirguis JEB, Mehanny SSF. Erratum for "evaluating code criteria for regular seismic behavior of continuous concrete box girder bridges with unequal height piers" by J. E. B. Guirguis and S. S. F. Mehanny. *J Bridge Eng* 2013;18:931. DOI
27. Wang X, Ye A, He Z, Shang Y. Quasi-static cyclic testing of elevated RC pile-cap foundation for bridge structures. *J Bridge Eng* 2016;21:04015042. DOI
28. Ismail M, Casas JR, Rodellar J. Near-fault isolation of cable-stayed bridges using RNC isolator. *Eng Struct* 2013;56:327-42. DOI
29. Xiang N, Alam MS. Displacement-based seismic design of bridge bents retrofitted with various bracing devices and their seismic fragility assessment under near-fault and far-field ground motions. *Soil Dyn Earthq Eng* 2019;119:75-90. DOI
30. Mazza F, Mazza M. Nonlinear seismic analysis of irregular r.c. framed buildings base-isolated with friction pendulum system under near-fault excitations. *Soil Dyn Earthq Eng* 2016;90:299-312. DOI
31. Chen X, Li C. Seismic performance of tall pier bridges retrofitted with lead rubber bearings and rocking foundation. *Eng Struct* 2020;212:110529. DOI
32. Chen X. System fragility assessment of tall-pier bridges subjected to near-fault ground motions. *J Bridge Eng* 2020;25:04019143. DOI
33. Nielson BG, DesRoches R. Seismic fragility methodology for highway bridges using a component level approach. *Earthq Eng Structl*

Dyn 2007;36:823-39. DOI

34. Padgett JE, Desroches R. Methodology for the development of analytical fragility curves for retrofitted bridges. *Earthq Eng Struct Dyn* 2008;37:1157-74. DOI
35. Zhang J, Huo Y. Evaluating effectiveness and optimum design of isolation devices for highway bridges using the fragility function method. *Eng Struct* 2009;31:1648-60. DOI
36. Zheng Y, Dong Y, Li Y. Resilience and life-cycle performance of smart bridges with shape memory alloy (SMA)-cable-based bearings. *Constr Build Mater* 2018;158:389-400. DOI
37. Alam MS, Bhuiyan MAR, Billah AHMM. Erratum to: seismic fragility assessment of SMA-bar restrained multi-span continuous highway bridge isolated by different laminated rubber bearings in medium to strong seismic risk zones. *Bull Earthq Eng* 2012;10:1911-3. DOI
38. Argyroudis SA, Nasiopoulos G, Mantadakis N, Mitoulis SA. Cost-based resilience assessment of bridges subjected to earthquakes. *Int J Disaster Resil Built Environ* 2021;12:209-22. DOI
39. Liu Y, Cao L, Yang D, Anderson BC. How social capital influences community resilience management development. *Environ Sci Policy* 2022;136:642-51. DOI
40. He X, Cha EJ. State of the research on disaster risk management of interdependent infrastructure systems for community resilience planning. *Sustain Resilient Infrastruct* 2022;7:391-420. DOI
41. Kunde M, Jangid R. Seismic behavior of isolated bridges: a-state-of-the-art review. *Electron J Struct Eng* 2003;3:140-70. DOI
42. Forcellini D, Alzabeebee S. Seismic fragility assessment of geotechnical seismic isolation (GSI) for bridge configuration. *Bull Earthq Eng* 2023;21:3969-90. DOI